38. M. S. Song *et al.*, *Nature* **455**, 813 (2008).
39. A. Sabo, M. Lusic, A. Cereseto, M. Giacca, *Mol. Cell. Biol.* **28**, 2201 (2008).
40. J. Zhang *et al.*, *Mol. Cell* **31**, 143 (2008).
41. H. Chen, R. J. Lin, W. Xie, D. Wilpitz, R. M. Evans, *Cell* **98**, 675 (1999).
42. R. Mahajan, C. Delphin, T. Guan, L. Gerace, F. Melchior, *Cell* **88**, 97 (1997).
43. S. Westermann, K. Weber, *Nat. Rev. Mol. Cell Biol.* **4**, 938 (2003).
44. X. Zhang *et al.*, *Mol. Cell* **27**, 197 (2007).
45. B. T. Scroggins *et al.*, *Mol. Cell* **25**, 151 (2007).
46. D. K. Morrison, *Trends Cell Biol.* **19**, 16 (2009).
47. X. Yang *et al.*, *Proc. Natl. Acad. Sci. U.S.A.* **103**, 17237 (2006).
48. K. Rittinger *et al.*, *Mol. Cell* **4**, 153 (1999).
49. X. Tang *et al.*, *Cell* **131**, 93 (2007).
50. We thank the members of the Department of Proteomics and Signal Transduction at the Max Planck Institute for Biochemistry for their helpful discussions and suggestions; T. Hyman, I. Poser, and N. Hubner for providing GFP-tagged bacterial artificial chromosome (BAC) transgenic cell lines; J. Duyser and S. Raulefs for providing GST–14-3-3 expression plasmid; T. Misteli for providing CBX3 plasmid; Max Planck Institute for Biochemistry core facility for peptide synthesis and DNA sequencing; and H. Serve and C. Brandts for their advice with KDAC inhibitors. This work is supported by the Deutsche Krebshilfe (108401) and the Max Planck Society. M.L.N. is supported by the European Molecular Biology Organization.

Supporting Online Material
www.sciencemag.org/cgi/content/full/1175371/DC1
Materials and Methods
Figs S1 to S9
Tables S1 to S5
References

23 April 2009; accepted 30 June 2009
Published online 16 July 2009;
10.1126/science.1175371
Include this information when citing this paper.

Detection of 16 Gamma-Ray Pulsars Through Blind Frequency Searches Using the Fermi LAT

A. A. Abdo,[1]* M. Ackermann,[2] M. Ajello,[2] B. Anderson,[3] W. B. Atwood,[3] M. Axelsson,[4,5] L. Baldini,[6] J. Ballet,[7] G. Barbiellini,[8,9] M. G. Baring,[10] D. Bastieri,[11,12] B. M. Baughman,[13] K. Bechtol,[2] R. Bellazzini,[6] B. Berenji,[2] G. F. Bignami,[14] R. D. Blandford,[2] E. D. Bloom,[2] E. Bonamente,[15,16] A. W. Borgland,[2] J. Bregeon,[6] A. Brez,[6] M. Brigida,[17,18] P. Bruel,[19] T. H. Burnett,[20] G. A. Caliandro,[17,18] R. A. Cameron,[2] P. A. Caraveo,[21] J. M. Casandjian,[7] C. Cecchi,[15,16] Ö. Çelik,[22] A. Chekhtman,[1,23] C. C. Cheung,[22] J. Chiang,[2] S. Ciprini,[15,16] R. Claus,[2] J. Cohen-Tanugi,[24] J. Conrad,[4,25,26]† S. Cutini,[27] C. D. Dermer,[1] A. de Angelis,[28] A. de Luca,[14] F. de Palma,[17,18] S. W. Digel,[2] M. Dormody,[3]‡ E. do Couto e Silva,[2] P. S. Drell,[2] R. Dubois,[2] D. Dumora,[29,30] C. Farnier,[24] C. Favuzzi,[17,18] S. J. Fegan,[19] Y. Fukazawa,[31] S. Funk,[2] P. Fusco,[17,18] F. Gargano,[18] D. Gasparrini,[27] N. Gehrels,[22,32] S. Germani,[15,16] B. Giebels,[19] N. Giglietto,[17,18] P. Giommi,[27] F. Giordano,[17,18] T. Glanzman,[2] G. Godfrey,[2] I. A. Grenier,[7] M.-H. Grondin,[29,30] J. E. Grove,[1] L. Guillemot,[29,30] S. Guiriec,[33] C. Gwon,[1] Y. Hanabata,[31] A. K. Harding,[22] M. Hayashida,[2] E. Hays,[22] R. E. Hughes,[13] G. Jóhannesson,[2] R. P. Johnson,[3] T. J. Johnson,[22,32] W. N. Johnson,[1] T. Kamae,[2] H. Katagiri,[31] J. Kataoka,[34] N. Kawai,[35,36] M. Kerr,[20] J. Knödlseder[37] M. L. Kocian,[2] M. Kuss,[6] J. Lande,[2] L. Latronico,[6] M. Lemoine-Goumard,[29,30] F. Longo,[8,9] F. Loparco,[17,18] B. Lott,[29,30] M. N. Lovellette,[1] P. Lubrano,[15,16] G. M. Madejski,[2] A. Makeev,[1,23] M. Marelli,[21] M. N. Mazziotta,[18] W. McConville,[22,32] J. E. McEnery,[22] C. Meurer,[4,26] P. F. Michelson,[2] W. Mitthumsiri,[2] T. Mizuno,[31] C. Monte,[17,18] M. E. Monzani,[2] A. Morselli,[38] I. V. Moskalenko,[2] S. Murgia,[2] P. L. Nolan,[2] J. P. Norris,[39] E. Nuss,[24] T. Ohsugi,[31] N. Omodei,[6] E. Orlando,[40] J. F. Ormes,[39] D. Paneque,[2] D. Parent,[29,30] V. Pelassa,[24] M. Pepe,[15,16] M. Pesce-Rollins,[6] M. Pierbattista,[7] F. Piron,[24] T. A. Porter,[3] J. R. Primack,[3] S. Rainò,[17,18] R. Rando,[11,12] P. S. Ray,[1]‡ M. Razzano,[6] N. Rea,[41,42] A. Reimer,[2] O. Reimer,[2] T. Reposeur,[29,30] S. Ritz,[22] L. S. Rochester,[2] A. Y. Rodriguez,[42] R. W. Romani,[2] F. Ryde,[4,25] H. F.-W. Sadrozinski,[3] D. Sanchez,[19] A. Sander,[13] P. M. Saz Parkinson,[3]‡ J. D. Scargle,[43] C. Sgrò,[6] E. J. Siskind,[44] D. A. Smith,[29,30] P. D. Smith,[13] G. Spandre,[6] P. Spinelli,[17,18] J.-L. Starck,[7] M. S. Strickman,[1] D. J. Suson,[45] H. Tajima,[2] H. Takahashi,[31] T. Takahashi,[46] T. Tanaka,[2] J. G. Thayer,[2] D. J. Thompson,[22] L. Tibaldo,[11,12] O. Tibolla,[47] D. F. Torres,[42,48] G. Tosti,[15,16] A. Tramacere,[2,49] Y. Uchiyama,[2] T. L. Usher,[2] A. Van Etten,[2] V. Vasileiou,[50,51] N. Vilchez,[37] V. Vitale,[38,52] A. P. Waite,[2] P. Wang,[2] K. Watters,[2] B. L. Winer,[13] M. T. Wolff,[1] K. S. Wood,[1] T. Ylinen,[4,25,53] M. Ziegler[3]‡

Pulsars are rapidly rotating, highly magnetized neutron stars emitting radiation across the electromagnetic spectrum. Although there are more than 1800 known radio pulsars, until recently only seven were observed to pulse in gamma rays, and these were all discovered at other wavelengths. The Fermi Large Area Telescope (LAT) makes it possible to pinpoint neutron stars through their gamma-ray pulsations. We report the detection of 16 gamma-ray pulsars in blind frequency searches using the LAT. Most of these pulsars are coincident with previously unidentified gamma-ray sources, and many are associated with supernova remnants. Direct detection of gamma-ray pulsars enables studies of emission mechanisms, population statistics, and the energetics of pulsar wind nebulae and supernova remnants.

A wide variety of astrophysical phenomena, such as black holes, active galactic nuclei, gamma-ray bursts, and pulsars, are known to produce photons with energies exceeding tens of megaelectron volts. Detection and accurate localization of sources at these energies is challenging because of the low fluxes involved and the limitations of the detection techniques. The sky above 100 MeV was surveyed more than 30 years ago by the COS-B satellite (*1*) and more recently by the Energetic Gamma Ray Experiment Telescope (EGRET) (*2*) onboard the Compton Gamma Ray Observatory. One of the main legacies of EGRET was the detection of ~300 gamma-ray sources, many of which have remained unidentified despite searches at a wide variety of wavelengths (*3*). Many EGRET (and COS-B) unidentified sources are thought to be of galactic origin because of their lack of variability and concentration along the galactic plane. A large fraction of these have been suspected to be pulsars [e.g., (*4*–*6*)] despite deep radio and x-ray searches often failing to uncover pulsed emission, even when the gamma-ray sources were coincident with supernova remnants (SNRs) or pulsar wind nebulae (PWNs). The lack of radio pulsations has usually been explained as the narrow radio beams missing the line of sight toward Earth (*7*). We refer to such pulsars as "radio-quiet"; even though they may emit radio waves, these cannot be detected at Earth. Before the launch of the Fermi Gamma-ray Space Telescope, Geminga (*8*) was the only known radio-quiet gamma-ray pulsar. Current models of pulsar gamma-ray emission predict that gamma-ray beams are much wider than radio beams (*9*), thus suggesting that there may be a large population of radio-quiet gamma-ray pulsars.

Soon after launch on 11 June 2008, the Large Area Telescope (LAT) onboard Fermi began surveying the sky at energies above 20 MeV. A companion paper describes the LAT detection of a population of gamma-ray millisecond pulsars (MSPs) (*10*). Here we report the detection of 16 pulsars found in blind frequency searches using the LAT. Previously, gamma-ray pulsars had been detected only with the use of a radio (or, in the case of Geminga, an x-ray) ephemeris.

Observations and data analysis. The LAT is a high-energy gamma-ray telescope sensitive to photon energies from 20 MeV to >300 GeV, featuring a solid-state silicon tracker, a cesium-iodide calorimeter, and an anticoincidence detector (*11*). Gamma-ray events recorded in the LAT have time stamps derived from a GPS clock on the Fermi satellite with an accuracy of <1 μs (*12*). The LAT operates in continuous sky survey mode, covering the entire sky every 3 hours. Relative to EGRET, the LAT has a larger effective area (9500 cm^2 at normal incidence), larger field of view (2.4 sr), more efficient use of time on orbit for photon collection, and a finer point spread function (5° at 100 MeV, 0.8° at 1 GeV). The first three factors result in more rapid photon accumulation, and the fourth increases the signal-to-noise ratio by improving the background rejection.

Table 1. Names and locations of the gamma-ray pulsars discovered in our blind searches. The "assumed counterpart" column is the x-ray source that provided the position for the timing model, which in some cases may not be the true counterpart; *l* and *b* are galactic longitude and latitude, respectively.

LAT PSR	LAT source 0FGL	EGRET source	Assumed counterpart	RA (°)	Dec (°)	*l* (°)	*b* (°)
J0007+7303	J0007.4+7303	3EG J0010+7309	RX J0007.0+7303 in G119.5+10.3 (*37*)	1.7565	73.0523	119.7	10.5
J0357+32	J0357.5+3205			59.445	32.105	162.7	−16.0
J0633+0632	J0633.5+0634	3EG J0631+0642	Swift J063343.8+063223	98.4333	6.5403	205.1	−0.9
J1418−6058	J1418.8−6058	3EG J1420−6038	R1 in G313.3+0.1 (*24*)	214.6779	−60.9675	313.3	0.1
J1459−60	J1459.4−6056			224.874	−60.878	317.9	−1.8
J1732−31	J1732.8−3135	3EG J1734−3232		263.169	−31.610	356.2	0.9
J1741−2054	J1742.1−2054	3EG J1741−2050	Swift J174157.8−205412	265.4908	−20.9033	6.4	4.9
J1809−2332	J1809.5−2331	3EG J1809−2328	CXOU J180950.2−233223 in G7.4−2.0 (*38*)	272.4592	−23.5397	7.4	−2.0
J1813−1246	J1813.5−1248	GeV J1814−1228	Swift J181323.4−124600	273.3475	−12.7668	17.2	2.4
J1826−1256	J1825.9−1256	3EG J1826−1302	AXJ1826.1−1257 in G18.5−0.4 (*26*)	276.5356	−12.9429	18.6	−0.4
J1836+5925	J1836.2+5924	3EG J1835+5918	RX J1836.2+5925 (*30*)	279.0570	59.4250	88.9	25.0
J1907+06	J1907.5+0602	GeV J1907+0557		286.965	6.022	40.2	−0.9
J1958+2846	J1958.1+2848	3EG J1958+2909	Swift J195846.1+284602	299.6921	28.7674	65.9	−0.4
J2021+4026	J2021.5+4026	3EG J2020+4017	S21 in G78.2+2.1 (*33*)	305.3777	40.4462	78.2	2.1
J2032+4127	J2032.2+4122	3EG J2033+4118	MT91 221 in Cygnus OB2 (*32*)	308.0612	41.4610	80.2	1.0
J2238+59	—			339.561	59.080	106.5	0.5

Even with the improvements of the LAT, gamma-ray data remain extremely sparse. The brightest steady gamma-ray source in the sky, the Vela pulsar, spins 11 times per second; however, it provides fewer than 100 (>30 MeV) photons during every two orbits of the LAT (*13*). As a result, detection of gamma-ray pulsations from sources with more typical brightness requires weeks or months of data. A standard technique for finding a periodic signal in a data set is a fast Fourier transform (FFT). A fully coherent FFT becomes memory-intensive because the number of frequency bins in the FFT increases with the length of the observational time: $N_{\mathrm{bins}} = 2Tf_{\mathrm{max}}$, where T is the duration of the observation and f_{max} is the maximum frequency. Furthermore, pulsars gradually spin down as they radiate away energy, requiring the computation of many tens of thousands of FFTs to scan a realistic frequency and frequency derivative (f and $\dot{f}$) parameter space; this makes FFT searches computationally intensive, if not prohibitive [e.g., (*14*)]. We thus used the time-differencing technique (*15*) and a fixed window of $T = 2^{19}$ s (~1 week). This markedly reduces the number of FFT bins and frequency derivative trials. This method was successfully applied to EGRET data (*16*).

We applied the time-differencing technique to photons from a small region of interest around selected target positions. We used two sets of target positions. The first was a list of ~100 promising locations derived from multiwavelength observations. This list was selected on the basis of location in the galactic plane, spectra, lack of long-term variability, and presence of an SNR, a PWN, or a likely neutron star identified from x-ray observations. Many of these locations were unidentified gamma-ray sources from EGRET. The second list, compiled after the LAT started collecting data, included locations of gamma-ray sources from a preliminary version of the LAT catalog. After eliminating sources with probable active galactic nuclei associations, we ended up with ~200 locations, of which 36 were consistent with previously unidentified EGRET sources.

We analyzed data collected from sky survey observations beginning on 4 August 2008 and ending on 25 December 2008. We applied a barycenter correction using the JPL DE405 solar system ephemeris (*17*), assuming that the source position was either a likely candidate counterpart, found through multiwavelength studies, or our best estimate based on LAT data. This translation into the nearly inertial reference frame of the solar system barycenter corrects

[1]Space Science Division, Naval Research Laboratory, Washington, DC 20375, USA. [2]W. W. Hansen Experimental Physics Laboratory, Kavli Institute for Particle Astrophysics and Cosmology, Department of Physics and SLAC National Accelerator Laboratory, Stanford University, Stanford, CA 94305, USA. [3]Santa Cruz Institute for Particle Physics, Department of Physics and Department of Astronomy and Astrophysics, University of California, Santa Cruz, CA 95064, USA. [4]Oskar Klein Centre for Cosmo Particle Physics, AlbaNova, SE-106 91 Stockholm, Sweden. [5]Department of Astronomy, Stockholm University, SE-106 91 Stockholm, Sweden. [6]Istituto Nazionale di Fisica Nucleare, Sezione di Pisa, I-56127 Pisa, Italy. [7]Laboratoire AIM, CEA-IRFU/CNRS/Université Paris Diderot, Service d'Astrophysique, CEA Saclay, 91191 Gif-sur-Yvette, France. [8]Istituto Nazionale di Fisica Nucleare, Sezione di Trieste, I-34127 Trieste, Italy. [9]Dipartimento di Fisica, Università di Trieste, I-34127 Trieste, Italy. [10]Department of Physics and Astronomy, Rice University, Houston, TX 77251, USA. [11]Istituto Nazionale di Fisica Nucleare, Sezione di Padova, I-35131 Padova, Italy. [12]Dipartimento di Fisica "G. Galilei," Università di Padova, I-35131 Padova, Italy. [13]Department of Physics, Center for Cosmology and Astro-Particle Physics, Ohio State University, Columbus, OH 43210, USA. [14]Istituto Universitario di Studi Superiori, I-27100 Pavia, Italy. [15]Istituto Nazionale di Fisica Nucleare, Sezione di Perugia, I-06123 Perugia, Italy. [16]Dipartimento di Fisica, Università degli Studi di Perugia, I-06123 Perugia, Italy. [17]Dipartimento di Fisica "M. Merlin" dell'Università e del Politecnico di Bari, I-70126 Bari, Italy. [18]Istituto Nazionale di Fisica Nucleare, Sezione di Bari, 70126 Bari, Italy. [19]Laboratoire Leprince-Ringuet, École Polytechnique, CNRS/IN2P3, Palaiseau, France. [20]Department of Physics, University of Washington, Seattle, WA 98195, USA. [21]INAF-Istituto di Astrofisica Spaziale e Fisica Cosmica, I-20133 Milano, Italy. [22]NASA Goddard Space Flight Center, Greenbelt, MD 20771, USA. [23]George Mason University, Fairfax, VA 22030, USA. [24]Laboratoire de Physique Théorique et Astroparticules, Université Montpellier 2, CNRS/IN2P3, Montpellier, France. [25]Department of Physics, Royal Institute of Technology (KTH), AlbaNova, SE-106 91 Stockholm, Sweden. [26]Department of Physics, Stockholm University, AlbaNova, SE-106 91 Stockholm, Sweden. [27]Agenzia Spaziale Italiana (ASI) Science Data Center, I-00044 Frascati (Roma), Italy. [28]Dipartimento di Fisica, Università di Udine and Istituto Nazionale di Fisica Nucleare, Sezione di Trieste, Gruppo Collegato di Udine, I-33100 Udine, Italy. [29]CNRS/IN2P3, Centre d'Études Nucléaires Bordeaux Gradignan, UMR 5797, 33175 Gradignan, France. [30]Université de Bordeaux, Centre d'Études Nucléaires Bordeaux Gradignan, UMR 5797, 33175 Gradignan, France. [31]Department of Physical Sciences, Hiroshima University, Higashi-Hiroshima, Hiroshima 739-8526, Japan. [32]University of Maryland, College Park, MD 20742, USA. [33]University of Alabama, Huntsville, AL 35899, USA. [34]Waseda University, 1-104 Totsukamachi, Shinjuku-ku, Tokyo, 169-8050, Japan. [35]Cosmic Radiation Laboratory, Institute of Physical and Chemical Research (RIKEN), Wako, Saitama 351-0198, Japan. [36]Department of Physics, Tokyo Institute of Technology, Meguro City, Tokyo 152-8551, Japan. [37]Centre d'Étude Spatiale des Rayonnements, CNRS/UPS, BP 44346, F-30128 Toulouse Cedex 4, France. [38]Istituto Nazionale di Fisica Nucleare, Sezione di Roma "Tor Vergata," I-00133 Roma, Italy. [39]Department of Physics and Astronomy, University of Denver, Denver, CO 80208, USA. [40]Max-Planck-Institut für Extraterrestrische Physik, 85748 Garching, Germany. [41]Sterrenkundig Institut "Anton Pannekoek," 1098 SJ Amsterdam, Netherlands. [42]Institut de Ciencies de l'Espai (IEEC-CSIC), Campus UAB, 08193 Barcelona, Spain. [43]Space Sciences Division, NASA Ames Research Center, Moffett Field, CA 94035, USA. [44]NYCB Real-Time Computing Inc., Lattingtown, NY 11560, USA. [45]Department of Chemistry and Physics, Purdue University Calumet, Hammond, IN 46323, USA. [46]Institute of Space and Astronautical Science, JAXA, 3-1-1 Yoshinodai, Sagamihara, Kanagawa 229-8510, Japan. [47]Max-Planck-Institut für Kernphysik, D-69029 Heidelberg, Germany. [48]Institució Catalana de Recerca i Estudis Avançats, Barcelona, Spain. [49]Consorzio Interuniversitario per la Fisica Spaziale, I-10133 Torino, Italy. [50]Center for Research and Exploration in Space Science and Technology, NASA Goddard Space Flight Center, Greenbelt, MD 20771, USA. [51]University of Maryland, Baltimore County, Baltimore, MD 21250, USA. [52]Dipartimento di Fisica, Università di Roma "Tor Vergata," I-00133 Roma, Italy. [53]School of Pure and Applied Natural Sciences, University of Kalmar, SE-391 82 Kalmar, Sweden.

*National Research Council Research Associate.
†Royal Swedish Academy of Sciences Research Fellow, funded by a grant from the K. A. Wallenberg Foundation.
‡To whom correspondence should be addressed. E-mail: dormody@scipp.ucsc.edu (M.D.); paul.ray@nrl.navy.mil (P.S.R.); pablo@scipp.ucsc.edu (P.M.S.P.); ziegler@scipp.ucsc.edu (M.Z.)

for classical and relativistic effects of the motion of Earth. We accepted all highest-quality ["diffuse" class (*11*)] photons falling within a 0.8° radius of our source location with energies greater than 300 MeV. For each target, we searched a set of trial frequency derivatives from zero to the spin-down of the young Crab pulsar ($\dot{f} = -3.7 \times 10^{-10}$ Hz s^{-1}). For each trial, we corrected the photon arrival times using the assumed frequency derivative, calculated the time differences, computed the FFT sampled with a Nyquist frequency of 64 Hz, and searched the spectrum for significant peaks.

We refined candidate signals by performing an epoch-folding search over a narrow region of frequency and frequency-derivative space using PRESTO (*18*). Using the parameters from the time-differencing search as an initial timing model, we split the data into intervals (~2 to 4 weeks, depending on signal-to-noise ratio), and measured pulse times of arrival (TOAs) in each segment. These TOAs were fit to a timing model with the Tempo2 pulsar timing package (*19*). We selected the reference epoch for all timing models to be MJD (modified Julian date) 54754.0, roughly in the middle of the observation interval.

Table 2. Rotational ephemerides for the new pulsars. For all timing solutions, the reference epoch is MJD 54754. The given frequency and frequency derivative are barycentric. Numbers in parentheses indicate error in the last significant digit(s). For LAT PSR J0357+32, marked with (†), the measured frequency derivative, and thus the derived parameters, may be significantly affected by positional error (see text). We also list the number of photons, n_γ, obtained with the cuts used in this work (see text) over the 5-month observational period. The 1- to 100-GeV photon number flux, F_{35}, is given, as presented in the Fermi Bright Source List (*39*), except for LAT PSR J2238+59, which was not in the Bright Source List but whose flux was derived from the same data set and analysis approach.

LAT PSR	n_γ	F_{35} (10^{-8} cm^{-2} s^{-1})	f (Hz)	$\dot{f}$ (-10^{-12} Hz s^{-1})	τ (years)	$\dot{E}$ (10^{34} ergs s^{-1})	B (10^{12} G)
J0007+7303	1509	6.14(27)	3.1658891845(5)	3.6133(3)	13,900	45.2	10.8
J0357+32	294	0.64(10)	2.251723430(1)	0.0610(9)†	585,000	0.5	2.3
J0633+0632	648	1.60(17)	3.3625440117(3)	0.8992(2)	59,300	11.9	4.9
J1418–6058	3160	5.42(38)	9.0440257591(8)	13.8687(5)	10,300	495.2	4.4
J1459–60	1089	1.26(19)	9.694596648(2)	2.401(1)	64,000	91.9	1.6
J1732–31	2843	3.89(33)	5.087952372(2)	0.677(1)	119,000	13.6	2.3
J1741–2054	889	1.31(17)	2.417211371(1)	0.0977(7)	392,000	0.9	2.7
J1809–2332	2606	5.63(31)	6.8125455291(4)	1.5975(3)	67,600	43.0	2.3
J1813–1246	1832	2.79(24)	20.802108713(5)	7.615(4)	43,300	625.7	0.9
J1826–1256	4102	5.76(37)	9.0726142968(4)	9.9996(3)	14,400	358.2	3.7
J1836+5925	2076	8.36(31)	5.7715516964(9)	0.0508(6)	1,800,000	1.2	0.5
J1907+06	2869	3.74(29)	9.378101746(2)	7.682(1)	19,400	284.4	3.1
J1958+2846	1355	1.29(18)	3.443663690(2)	2.493(1)	21,900	33.9	7.9
J2021+4026	4136	10.60(40)	3.769079109(1)	0.7780(7)	76,800	11.6	3.9
J2032+4127	2371	3.07(26)	6.9809351235(8)	0.9560(4)	115,800	26.3	1.7
J2238+59	811	0.96(11)	6.145017519(3)	3.722(2)	26,200	90.3	4.1

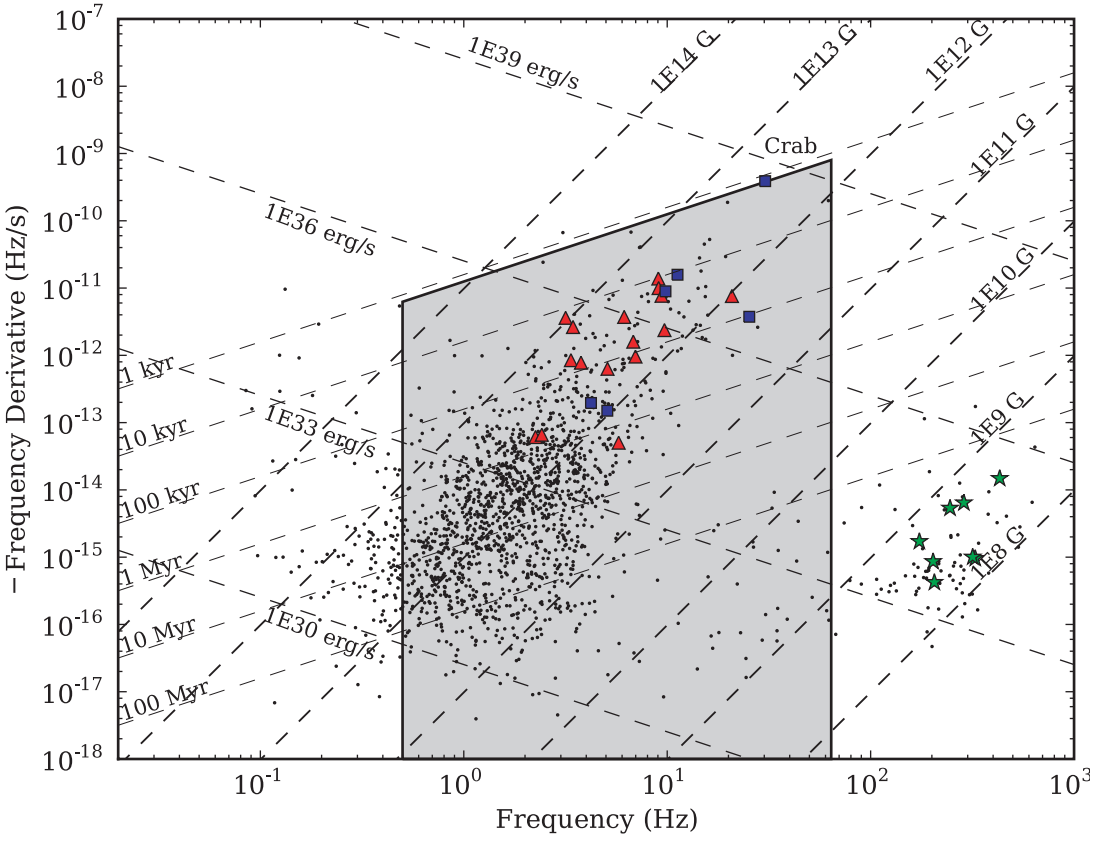

Fig. 1. Frequency (f) and frequency derivative ($\dot{f}$) distribution of the new pulsars. The dots represent the ~1800 pulsars in the ATNF catalog (*20*), the triangles represent the new pulsars reported here, and the squares represent the six previously known EGRET gamma-ray pulsars, including the Crab. The stars represent the new population of gamma-ray millisecond pulsars detected by the Fermi LAT and reported in (*10*). The shaded region shows the parameter space covered by our blind search and includes ~86% of the ATNF pulsars. The three sets of lines illustrate the characteristic age $\tau = -f/2\dot{f}$, inferred surface magnetic field strength $B = 3.2 \times 10^{19}\sqrt{-\dot{f}/f^3}$ G, and spin-down power given by $\dot{E} = 4\pi^2 I f \dot{f}$ ergs s^{-1}, where I is the neutron star moment of inertia ($I = 10^{45}$ g·cm^2). This figure shows that the blind-search gamma-ray pulsars are drawn from the portion of the general population with the highest spin-down luminosity.

This choice minimized the covariances between the timing model parameters. We identified 16 pulsars within the first 4 months of data, and confirmed these with the use of an independent data set of at least 1 additional month (Figs. 1 and 2; Tables 1 and 2).

Six of the 16 pulsars were found using the positions of well-localized counterparts at other wavelengths, whereas 10 were found using LAT source positions. The LAT positions were uncertain by several arc minutes, and in many cases the initial timing models showed very large nonwhite residuals indicative of a significant distance between the true position and the position being used to barycenter the data. We refined the positions in several ways (see below). The number of digits used in the declination of the names assigned to the pulsars reflects our confidence in their localization. The discovery frequency may not be the true pulsar rotation frequency, but rather a harmonic or a subharmonic, especially for gamma-ray pulse profiles with two peaks separated by ~180° in phase. We tested for this effect, but for certain cases (e.g., J0357+32) the results remain inconclusive because of the low photon counts.

The gamma-ray pulsars. The 16 pulsars are representative of the highest spin-down luminosity portion of the general population, which includes 1800 pulsars in the Australia Telescope National Facility (ATNF) database (*20*), including the six gamma-ray pulsars detected with EGRET, as well as eight gamma-ray MSPs detected by the Fermi LAT (*10*).

Thirteen LAT pulsars are associated with unidentified EGRET sources. Indeed, 15 of 36 unidentified EGRET sources searched showed pulsations, although two of them (PSR J1028–5819 and PSR J2021+3651) are known radio pulsars (*21*, *22*). Three pulsars (J0357+32, J1459–60, and J2238+59) correspond to newly seen LAT sources. This result suggests that the blind searches are flux-limited; although many LAT unidentified sources also could be pulsars, most have too low a flux for a pulsation to have been detected in our available data. Five pulsars are likely associated with PWNs and/or SNRs, and an additional one (J1836+5925) is associated with a known isolated neutron star. J0007+7303 (*23*) was long suspected of being a pulsar because of its clear association with SNR CTA 1 containing a PWN. J1418–6058 is in the complex Kookaburra region of the galactic plane and is likely associated with PWN

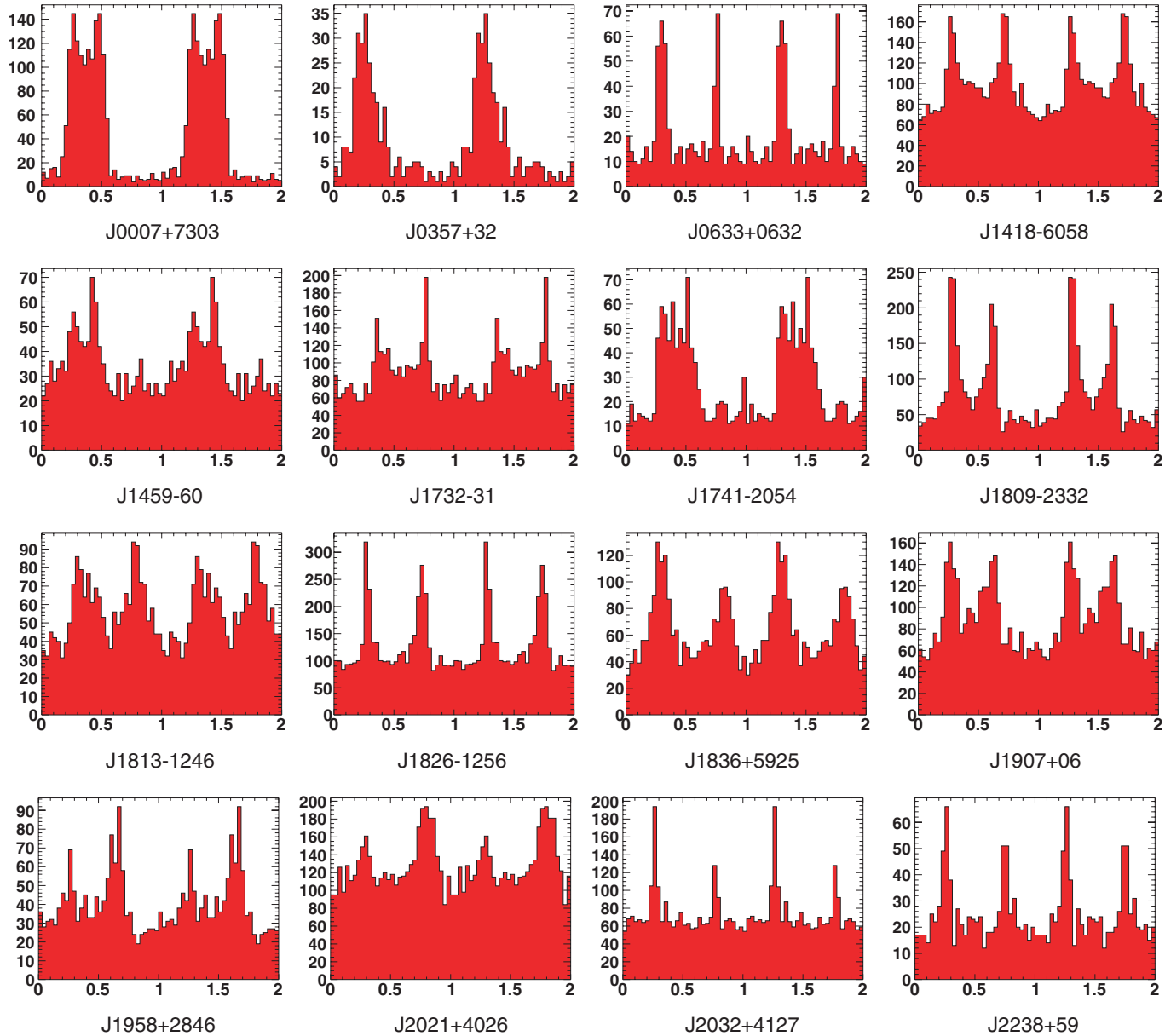

Fig. 2. Folded light curves, with a resolution of 32 phase bins per period, of the 16 pulsars discovered with the Fermi LAT, using 5 months of data with $E >$ 300 MeV, selected from a region of radius 0.8° around the best position for the pulsar. The light curves are not background-subtracted and can include a substantial contribution from the galactic diffuse gamma-ray emission, particularly for the pulsars at low galactic latitude. The *x* axis represents phase; the *y* axis represents counts per phase bin. Two rotations are shown, and the phase of the first peak has been placed at ~0.3 for clarity.

G313.3+0.1, the "Rabbit" (*24*). J1809–2332, likely powering the "Taz" PWN, is also possibly associated with a recently discovered mixed-morphology SNR, G7.5–1.7 (*25*). J1826–1256 is probably powering the "Eel" PWN (*26*), whereas J2021+4026 reveals that a pulsar is present, as long suspected, inside the γ Cygni SNR (*27*). Two more pulsars present plausible associations with SNRs: J0633+0632 is in the fairly old (~30,000 years) complex Monoceros Loop SNR (G205.5+0.5) at a distance of ~1.5 kpc (*28*), and J1907+06 is ~0.3° from SNR G40.5–0.5, but additional evidence is needed before an association can be demonstrated. J1836+5925 is the long-sought pulsar powering 3EG J1835+5918, the brightest and most accurately positioned of the unidentified EGRET sources off the plane (*29*). Our pulsar coincides with RX J1836+5925, an isolated neutron star for which x-ray pulsations were extensively searched but not found (*30*). Deep radio pulsation searches with the Green Bank Telescope at the National Radio Astronomy Observatory placed an upper limit at 1.4 GHz on flux density of 7 μJy for a spin period $P \geq 10$ ms (*30*). The x-ray counterpart of 3EG J1835+5918 was already suspected to be similar to Geminga, just a bit older and slightly farther away [within ~800 pc (*31*)]. Using ~130 ks of publicly available Chandra High Resolution Camera x-ray observations of RX J1836.2+5925 [the same data searched by (*30*)], we searched for x-ray pulsations using our gamma-ray ephemeris, but found none. In addition to J1836+5925, three other pulsars are located off the plane, at $|b| > 3°$ (J0007+7303, J0357+32, and J1741–2054), whereas the remaining 12 are located in the galactic plane.

We imaged the error boxes of nine pulsars with specifically targeted short (~5 ks) Swift observations, and in four cases identified x-ray point sources within the LAT error circle that may be the x-ray counterparts (J0633+0632, J1741–2054, J1813–1246, and J1958+2846). In one other case, J2032+4127, Chandra observations (*32*) have revealed a number of x-ray point sources in the region. The best timing solution was found assuming the position of MT91 221, but this cannot be the true x-ray counterpart because it is known to be a B star. The region around J1418–6058 was mapped in detail by Chandra (*24*), and a promising point source, denoted R1, is consistent with the LAT source position and is likely the x-ray counterpart to the pulsar. Chandra observations of 3EG 2020+4017 show several possible counterparts to J2021+4026, of which S21 (*33*) has the best timing solution and is also most consistent with the LAT source position. Other pulsars were better localized using grid searches (J1459–60 and J1732–31) or on-pulse photon analyses (J0357+32, J1907+0601, and J2238+59). In our grid searches, we scanned 25 equally spaced locations overlapping the 95% LAT error circle, and looked for the position with the best timing solution. In on-pulse photon analyses, we used only the on-pulse photons to improve the source position.

Five pulsars suffer from large (~0.1°) positional uncertainties, which degrade the frequency derivative in the timing solution. The problem is particularly acute in J0357+32 (Table 2), and the ~5′ uncertainty in its position results in an uncertainty in the true value of the frequency derivative of $\sim 6 \times 10^{-14}$. Any parameters derived from its timing solution are not reliable.

Implications. Data from EGRET, COS-B, and SAS-2 demonstrated that rotation-powered pulsars are persistent sources of pulsed gamma rays. EGRET results also showed that the luminosity of detected pulsars over all wavelengths was dominated by the gamma-ray part of the spectrum. EGRET further established a list of persistent sources at low and intermediate galactic latitudes that could not be demonstrated to show pulsations. The Fermi LAT data confirm most of these sources and reveal that many of these persistent galactic gamma-ray sources are pulsars. Of 36 LAT sources with EGRET counterparts that were searched, 15 show pulsations (13 from previously unknown pulsars).

Until the launch of Fermi, the only known radio-quiet pulsar was Geminga, at a distance of ~250 pc (*34*) and with a spin-down luminosity of 3.2×10^{34} ergs s^{-1} and a gamma-ray efficiency of a few percent (for a 1-sr beam) or 50% (for isotropic emission) (*8*). It was already apparent ~30 years ago, as shown by COS-B observations (*1*), that the average unidentified gamma-ray source should have a luminosity greater than 10^{35} ergs s^{-1} to be consistent with the very narrow distribution of low-latitude gamma-ray sources (*4*, *35*). Later studies with EGRET confirmed this (*5*), showing that most unidentified sources were at ~1.2 to 1.6 kpc and had luminosities of 0.7×10^{35} to 16.7×10^{35} ergs s^{-1}. Thus, most unidentified sources could not be like Geminga [e.g., (*8*)]. The detection of mostly high-luminosity, low–galactic latitude, and probably relatively distant pulsars by the LAT confirms the predictions that the unidentified gamma-ray sources could not all be nearby, low-luminosity pulsars such as Geminga.

This new population of gamma-ray selected pulsars helps to reveal the geometry of emission from rotation-powered pulsars. A broad gamma-ray beam is required for at least part of our population of pulsars, as we see the high-energy beam but not the relatively narrow radio beam. Thus, this population favors pulsar emission models in which the high-energy radiation occurs in the outer magnetosphere, nearer to the light cylinder. Outer gap models [e.g., (*6*)], where particles are accelerated and radiate in vacuum gaps in the outer magnetosphere, and slot gap models [e.g., (*36*)], where particles are accelerated and radiate at all altitudes along the open magnetic field boundary, both can reproduce the wide, double-peaked light curves we observed (*9*).

References and Notes

1. B. N. Swanenburg *et al.*, *Astrophys. J.* **243**, L69 (1981).
2. R. C. Hartman *et al.*, *Astrophys. J. Suppl. Ser.* **123**, 79 (1999).
3. D. J. Thompson, *Rep. Prog. Phys.* **71**, 116901 (2008).
4. D. J. Helfand, *Mon. Not. R. Astron. Soc.* **267**, 490 (1994).
5. R. Mukherjee *et al.*, *Astrophys. J.* **441**, L61 (1995).
6. I.-A. Yadigaroglu, R. W. Romani, *Astrophys. J.* **449**, 211 (1995).
7. K. T. S. Brazier, S. Johnston, *Mon. Not. R. Astron. Soc.* **305**, 671 (1999).
8. G. F. Bignami, P. A. Caraveo, *Annu. Rev. Astron. Astrophys.* **34**, 331 (1996).
9. K. P. Watters, R. W. Romani, P. Weltevrede, S. Johnston, *Astrophys. J.* **695**, 1289 (2009).
10. A. A. Abdo *et al.*, *Science* **325**, 848 (2009); published online 2 July 2009 (10.1126/science.1176113).
11. W. B. Atwood *et al.*, *Astrophys. J.* **697**, 1071 (2009).
12. Fermi LAT Collaboration, http://arxiv.org/abs/0904.2226 (2009).
13. A. A. Abdo *et al.*, *Astrophys. J.* **696**, 1084 (2009).
14. A. M. Chandler *et al.*, *Astrophys. J.* **556**, 59 (2001).
15. W. B. Atwood, M. Ziegler, R. P. Johnson, B. M. Baughman, *Astrophys. J.* **652**, L49 (2006).
16. M. Ziegler, B. M. Baughman, R. P. Johnson, W. B. Atwood, *Astrophys. J.* **680**, 620 (2008).
17. E. M. Standish, *Astron. Astrophys.* **336**, 381 (1998).
18. S. M. Ransom, thesis, Harvard University (2001).
19. G. Hobbs, R. Edwards, R. Manchester, *Mon. Not. R. Astron. Soc.* **369**, 655 (2006).
20. R. N. Manchester, G. B. Hobbs, A. Teoh, M. Hobbs, *Astrophys. J.* **129**, 1993 (2005).
21. A. A. Abdo *et al.*, *Astrophys. J.* **695**, L72 (2009).
22. A. A. Abdo *et al.*, *Astrophys. J.* **700**, 1059 (2009).
23. A. A. Abdo *et al.*, *Science* **322**, 1218 (2008); published online 16 October 2008 (10.1126/science.1165572).
24. C.-Y. Ng, M. S. E. Roberts, R. W. Romani, *Astrophys. J.* **627**, 904 (2005).
25. M. S. E. Roberts, C. L. Brogan, *Astrophys. J.* **681**, 320 (2008).
26. M. S. E. Roberts, R. W. Romani, N. Kawai, *Astrophys. J. Suppl. Ser.* **133**, 451 (2001).
27. K. T. S. Brazier, G. Kanbach, A. Carramiñana, J. Guichard, M. Merck, *Mon. Not. R. Astron. Soc.* **281**, 1033 (1996).
28. D. A. Leahy, S. Naranan, K. P. Singh, *Mon. Not. R. Astron. Soc.* **220**, 501 (1986).
29. O. Reimer *et al.*, *Mon. Not. R. Astron. Soc.* **324**, 772 (2001).
30. J. P. Halpern, F. Camilo, E. V. Gotthelf, *Astrophys. J.* **668**, 1154 (2007).
31. J. P. Halpern, E. V. Gotthelf, N. Mirabal, F. Camilo, *Astrophys. J.* **573**, L41 (2002).
32. R. Mukherjee, J. P. Halpern, E. V. Gotthelf, M. Eracleous, N. Mirabal, *Astrophys. J.* **589**, 487 (2003).
33. M. C. Weisskopf *et al.*, *Astrophys. J.* **652**, 387 (2006).
34. J. Faherty, F. M. Walter, J. Anderson, *Astrophys. Space Sci.* **308**, 225 (2007).
35. G. F. Bignami, W. Hermsen, *Annu. Rev. Astron. Astrophys.* **21**, 67 (1983).
36. A. K. Harding, J. V. Stern, J. Dyks, M. Frackowiak, *Astrophys. J.* **680**, 1378 (2008).
37. J. P. Halpern, E. V. Gotthelf, F. Camilo, D. J. Helfand, S. M. Ransom, *Astrophys. J.* **612**, 398 (2004).
38. T. M. Braje, R. W. Romani, M. S. E. Roberts, N. Kawai, *Astrophys. J.* **565**, L91 (2002).
39. A. A. Abdo *et al.*, *Astrophys. J. Suppl. Ser.* **183**, 46 (2009).

40. The Fermi LAT Collaboration is supported by NASA and the U.S. Department of Energy; the Commissariat à l'Energie Atomique and CNRS/Institut National de Physique Nucléaire et de Physique des Particules (France); the Agenzia Spaziale Italiana, Istituto Nazionale di Fisica Nucleare, and Istituto Nazionale di Astrofisica (Italy); the Ministry of Education, Culture, Sports, Science and Technology, High Energy Accelerator Research Organization (KEK), and Japan Aerospace Exploration Agency (Japan); and the K. A. Wallenberg Foundation, Swedish Research Council, and National Space Board (Sweden). Much of this work was carried out on the Pleiades supercomputer at the Department of Astronomy, University of California, Santa Cruz. This work made extensive use of the ATNF pulsar database. We thank N. Gehrels for granting Swift/XRT time to explore the LAT error circles, the Swift MOC staff for performing the observations, F. Camilo and S. Ransom for contributions, and M. Roberts for useful discussions.

Supporting Online Material

www.sciencemag.org/cgi/content/full/1175558/DC1
Fig. S1
References and Notes

29 April 2009; accepted 24 June 2009
Published online 2 July 2009;
10.1126/science.1175558
Include this information when citing this paper.